

*Supporting information*

**Supersorption capacity of anionic dye by newer chitosan hydrogel capsules via green surfactant exchange method**

Sudipta Chatterjee<sup>a</sup>, Hai Nguyen Tran<sup>b</sup>, Ohemeng-Boahen Godfred<sup>a</sup>, and Seung Han Woo<sup>a\*</sup>

*<sup>a</sup> Department of Chemical and Biological Engineering, Hanbat National University, 125 Dongseodaero, Yuseong-Gu, Daejeon 305-719, Republic of Korea*

*<sup>b</sup> Sustainable Management of Natural Resources and Environment Research Group, Faculty of Environment and Labour Safety, Ton Duc Thang University, Ho Chi Minh City, Vietnam*

---

\* Corresponding author:

Tel: +82 42 821 1537; fax: +82 42 821 1593; email: [shwoo@hanbat.ac.kr](mailto:shwoo@hanbat.ac.kr) (S.H. Woo)

## Section S1. Description of adsorption kinetic models

In this study, several kinetic models were applied to mathematically describe the intrinsic adsorption constants. The non-linearized forms of the pseudo-first-order [1], pseudo-second-order [2], and Elovich [3] models, are expressed in Equations 1, 2, and 3, respectively. The linear form of the intra-particle models [4] are given in Equation 4.

$$q_t = q_e(1 - e^{-k_1 t}) \quad (1)$$

$$q_t = \frac{q_e^2 k_2 t}{1 + k_2 q_e t} \quad (2)$$

$$q_t = \frac{1}{\beta} \ln(1 + \alpha \beta t) \quad (3)$$

$$q_t = k_{ip} \sqrt{t} + C \quad (4)$$

where  $k_1$  (1/min),  $k_2$  (g/mg×min),  $\alpha$  (mg/g × min), and  $k_{ip}$  (mg/g×min<sup>1/2</sup>) are the rate constants of the pseudo-first-order, pseudo-second-order, and intra-particle diffusion models, respectively;  $q_e$  and  $q_t$  are the adsorbate uptake per mass of adsorbent at equilibrium and at any time  $t$  (min), respectively;  $\beta$  (mg/g) is the desorption constant during any one experiment; and  $C$  (mg/g) is a constant describing the thickness of the boundary layer. Higher values of  $C$  correspond to a greater effect on the limiting boundary layer.

## Section S2. Description of adsorption isotherm models

In this study, the Langmuir (Eq. 5) [5], Freundlich (Eq. 6) [6], Redlich-Peterson (Eq. 7) [7], and Dubinin-Radushkevich (Eqs. 8–10) [8] models were employed to describe the adsorptive behavior of CR onto the capsules samples. To minimize the respective error functions, the non-linear optimization technique was applied for calculating the adsorption parameters from these models.

$$q_e = \frac{Q_{\max}^0 K_L C_e}{1 + K_L C_e} \quad (5)$$

$$q_e = K_F C_e^n \quad (6)$$

$$q_e = \frac{K_{RP} C_e}{1 + a_{RP} C_e^g} \quad (7)$$

$$q_e = q_{DR} e^{-K_{DR} \varepsilon^2} \quad (8)$$

$$\varepsilon = RT \ln\left(1 + \frac{1}{C_e}\right) \quad (9)$$

$$E = \frac{1}{\sqrt{2K_{DR}}} \quad (10)$$

where  $q_e$  (mg/g) is the amount of CR adsorbed onto capsule at equilibrium;  $C_e$  (mg/L) is the CR concentration at equilibrium;  $Q_{\max}^0$  (mg/g) is the maximum saturated monolayer adsorption capacity of adsorbent;  $K_L$  (L/mg) is the Langmuir constant related to the affinity between an adsorbent and adsorbate;  $K_F$  [(mg/g)/(L/mg)<sup>n</sup>] is the Freundlich constant, which characterizes the strength of adsorption;  $n$  (dimensionless) is a Freundlich intensity parameter;  $K_{RP}$  (L/g) and  $a_{RP}$  (mg/L)<sup>-g</sup> are the Redlich–Peterson constants;  $g$  (dimensionless) is an exponent whose value must lie between 0 and 1;  $q_{RD}$  (mg/g) is the adsorption capacity;  $K_{RD}$  (mol<sup>2</sup>/kJ<sup>2</sup>) is the constant related to the sorption energy;  $\varepsilon$  is the Polanyi potential; and  $E$  (kJ/mol) is the mean adsorption energy.

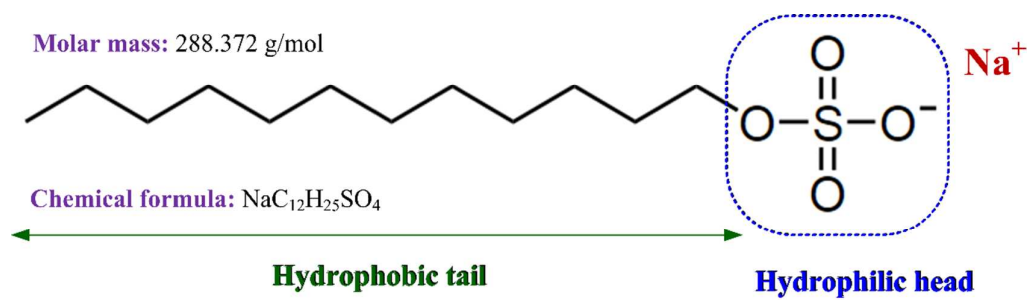


**Figure S1.** Chemical structure of sodium dodecyl sulfate

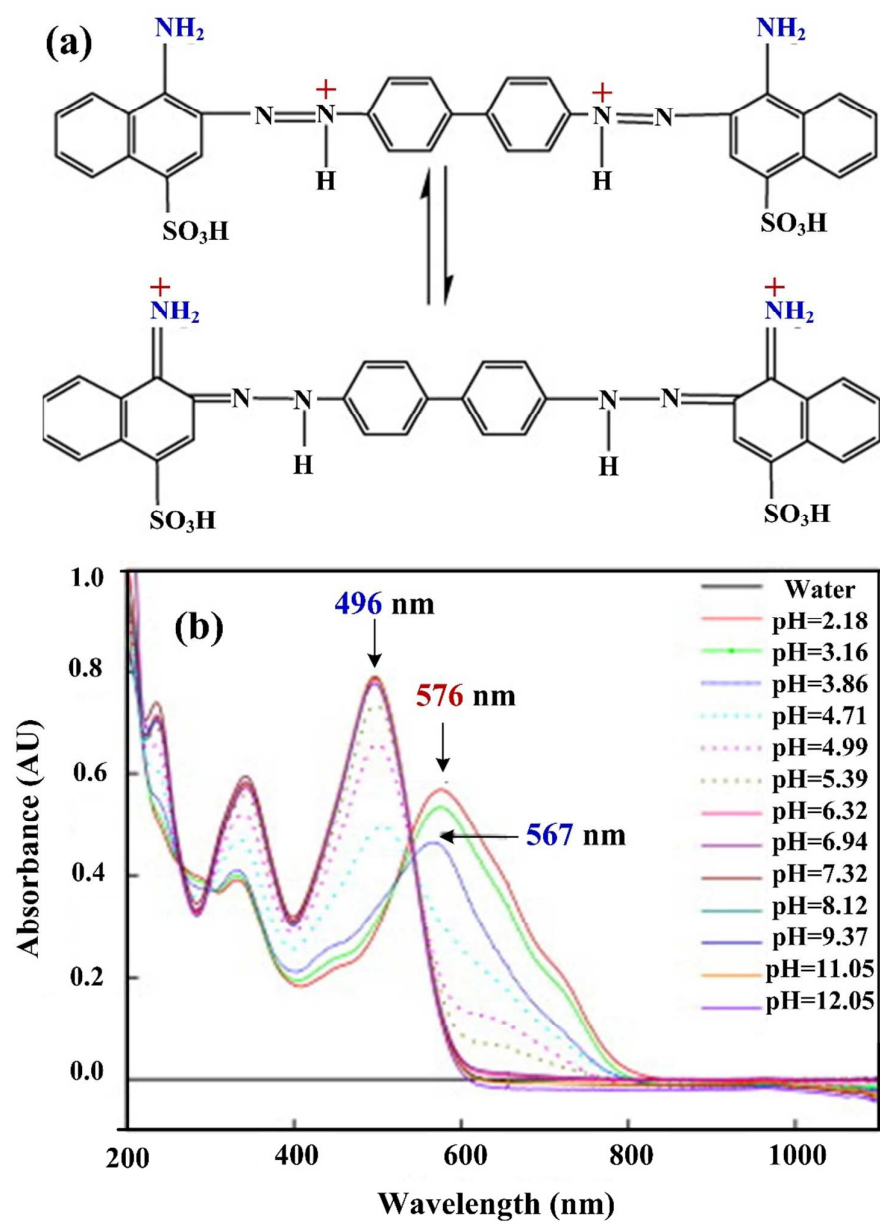


**Figure S2.** (a) Chemical structure of Congo Red and (b) UV-vis spectra of Congo Red solutions at different solution pH values [9])

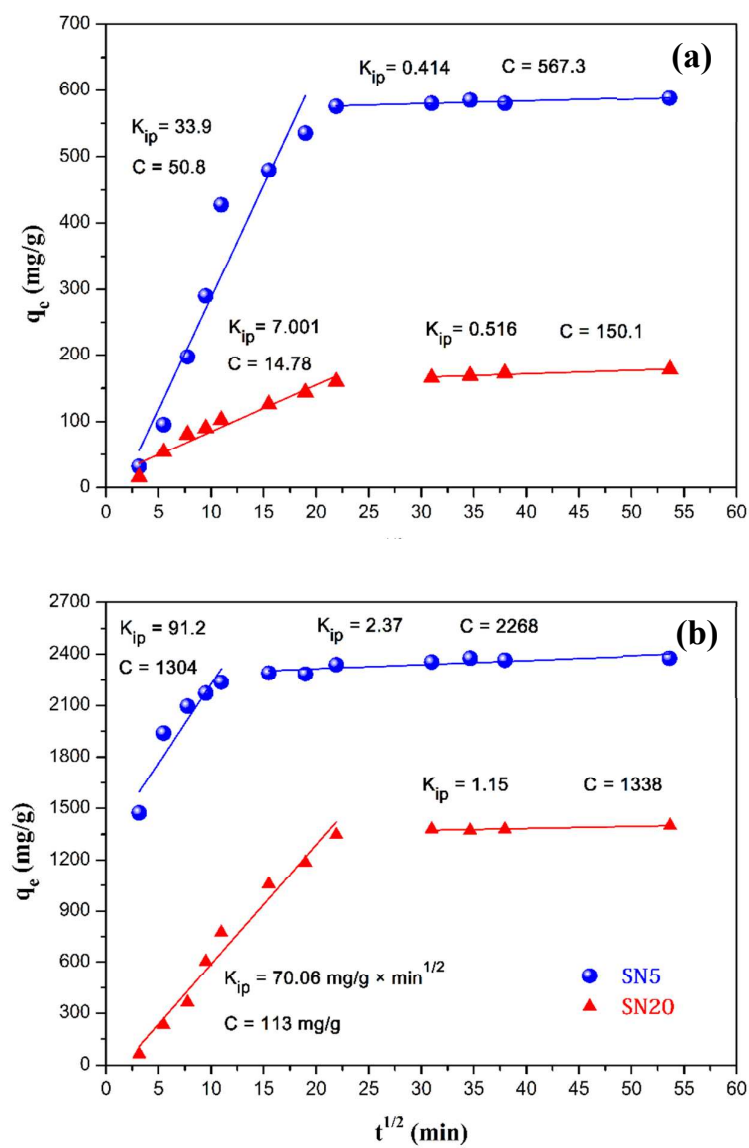


**Figure S3.** Intra-particle diffusion plot for CR adsorption of (a) pristine capsules (S5 and S20), and (b) NaOH-treated capsules (SN5 and SN20)

**Table S1.** Current treatment methods used to remove dye from effluents

<b>Technology</b>	<b>References</b>
Photodegradation or photocatalytic degradation	[10, 11]
Membrane	[12, 13]
Chemical coagulation and flocculation	[14-16]
Zonation	[16-18]
Biological treatment and biodegradation	[19, 20]
Adsorption	[21-23]
Advanced oxidation processes	[24, 25]
Electrochemical processes	[15, 26]
Ion exchange	[15, 27]

**Table S2.** Comparison of the maximum adsorption capacity (calculated from the Langmuir equation) of treated hydrogen capsules and other adsorbents reported in the literature

Adsorbent	Operation conditions				$Q^{\circ}_{\max}$ (mg/g)	Ref.
	$C_0$ (mg/L)	$t$ (h)	$T$ (°C)	pH		
Chitosan-based hydrogel capsule treated with NaOH (SN5 sample)	100–3000	30	24	5.0	<b>2592</b>	<b>This study</b>
<i>Biosorbents</i>						
Palm Kernel Seed Coat	30–150	2	30	6.7	66	[28]
Neem leaf powder	20–60	4	27	6.7	41	[29]
Jute stick powder	5–200	24	30	6.0	36	[30]
Wheat bran	50–300	8.3	25	8.0	23	[31]
Orange peel	10–100	1.5	29	7.7	22	[32]
Banana peel	10–150	2	30	7.9	18	[33]
Rice bran	50–300	8.3	25	8.0	15	[31]
Orange peel	10–150	2	30	7.9	14	[33]
<i>Biochar/Hydrochar</i>						
Rice straw biochar	50–5000	24	30	7.0	191	[34]
Wood chip biochar	50–5000	24	30	7.0	110	[34]
Bamboo hydrochar	5–100	12	25	NA	97	[35]
Korean cabbage biochar	50–5000	24	30	7.0	96	[34]
Residual algae biochar	30–200	2	27	7.0	51	[36]
Vermicompost biochar	5–200	6	25	7.0	31	[37]
<i>Activated carbon (AC)</i>						
Mesoporous carbon fibers	50–1000	24	Room	NA	1067	[38]
Silkworm cocoon AC fiber	10–400	10	Room	3.0	1100	[39]
Commercial AC	200–450	2	30	7.4	491	[40]
Commercial Darco® AC	50–5000	24	30	7.0	449	[34]
Straw AC	75–175	2	30	7.4	401	[40]
Commercial AC	50–200	12	30	7.0	300	[41]
Rice husk AC	75–175	2	30	7.4	238	[40]
Coconut shell AC	75–175	2	30	7.4	188	[40]
Groundnut shell AC	50–150	2	30	7.4	111	[40]
Bamboo dust AC	50–150	2	30	7.4	102	[40]
Bael shell carbon	40–80	3	30	5.7	98	[42]
<i>Layer double hydroxides (LDHs)</i>						
NMA-LDHs calcined at 600 °C	40–300	24	30	7.0	1250	[43]



(Ni/Mg/Al layered double oxides)						
Flower-like porous microspheres derived from Ni/Al-LDHs	10–500	48	25	NA	1229	[44]
Magnetic polydopamine Mg/Al LDH nano-flakes	30–150	4	20	5.6	585	[45]
Ni/Mg/Al LHHs hierarchical flower-like hollow microspheres	40–300	24	30	7.0	286	[43]
Mg–Fe–CO <sub>3</sub> –LDHs	5–50	1	25	4.0	105	[46]
Mg/Al–CO <sub>3</sub> –LDHs	10–200	1	Room	NA	37	[47]
<i><b>Zeolite and clay</b></i>						
Clay mixture	50–600	24	30	NA	575	[48]
Bentonite	75–300	2	25	6.8	159	[49]
Na-Bentonite	50–1000	12	30	7.5	36	[50]
Montmorillonite	25–100	12	30	7.0	13	[51]
Commercial Ceram kaolin	25–500	24	30	7.5	7.3	[52]
Commercial K15GR kaolin	25–500	24	30	7.5	6.8	[52]
Commercial Q38 kaolin	25–500	24	30	7.5	5.4	[52]
Kaolin	50–1000	24	30	7.5	5.4	[50]
Zeolite	50–1000	24	30	7.5	3.6	[50]
<i><b>Others</b></i>						
Carbon nanotube/Mg(Al)O nanocomposites	200–800	24	25	7.0	1250	[53]
Functionalized carbon nanotube	200–800	24	25	7.0	882	[53]
Fe(OH) <sub>3</sub> @Cellulose hybrid fibers	10–1000	24	25	NA	689	[54]
Chitosan hydrogel beads impregnated with carbon nanotubes	10–1000	24	30	5.0	450	[55]
Polyacrylamide-modified hydroxide aluminum/graphene composites (AGO)	100–500	12	35	3.0	424	[56]
Chitosan hydrogel beads impregnated with <i>cetyl trimethyl ammonium bromide</i>	10–1000	24	30	5.0	386	[57]
<i>N,O</i> -carboxymethyl-chitosan	200–1300	6	30	7.0	376	[58]
Sodium dodecylbenzene sulfonate modified-AGO	100–500	12	35	3.0	314	[56]
Cetyltrimethylammonium bromide modified -AGO	100–500	12	35	3.0	314	[56]
γ-Fe <sub>2</sub> O <sub>3</sub> nanorod	50–300	3	Room	5.0	233	[59]

Guar gum-graft-poly (acrylamide)/silica hybrid nanocomposite	10–200	2	35	3.0	221	[60]
Chito-hyr-bead with BDS	10–1000	24	30	5.0	209	[61]
Chito-hyr-bead with SDBS	10–1000	24	30	5.0	207	[61]
Hollow microspheres NiO–Si	10–100	20	30	7.0	204	[62]
Chito-hyr-bead with SDS	10–1000	24	30	5.0	186	[61]
Chitosan-based hydrogel beads	10–1000	24	30	5.0	183	[57]
Hollow microspheres Ni(OH) <sub>2</sub> –Si	10–100	20	30	7.0	114	[62]
Chito-hyr-bead with DSS	10–1000	24	30	5.0	114	[61]
FeC <sub>2</sub> O <sub>4</sub> .2H <sub>2</sub> O nanorod	50–300	3	Room	5.0	103	[59]
Chitosan	200–325	12	30	7.0	81	[51]
Chitosan	200–700	10	30	7.0	81	[58]
$\alpha$ -Fe <sub>2</sub> O <sub>3</sub> nanorod	50–300	3	Room	5.0	78	[59]
<i>N,O</i> -carboxymethyl-chitosan/montm orillonite nanocomposites	100–500	8	30	7.0	74	[63]
<i>p</i> TSA-Pani@GO-CNT nanocomposite	25–200	10	30	5.0	67	[64]
Cellulose/Fe <sub>3</sub> O <sub>4</sub> /AC composite	5–70	12	25	5.0	66	[65]
ZrO <sub>2</sub> hollow spheres	15–55	24	30	7.0	59	[66]
Chitosan/montmorillonite nanocomposites	100–225	12	30	7.0	55	[51]
CoFe <sub>1.93</sub> Gd <sub>0.07</sub> O <sub>4</sub>	25–120	3	20	NA	26	[67]
ZrO <sub>2</sub> solid spheres	15–55	24	30	7.0	21	[66]
ZrO <sub>2</sub> reagent	15–55	24	30	7.0	4.8	[66]

*NA: not adjusted*

Chito-hyr-bead (Chitosan hydrogel bead); SDS (sodium dodecyl sulfate); SDBS (dodecyl benzenesulfonic acid sodium salt); DS (sodium decyl sulfate), DSS (dioctyl sulfosuccinate sodium salt)

## References

1. Lagergren, S., *About the theory of so-called adsorption of soluble substances*. Kungliga Svenska Vetenskapsakademiens Handlingar, 1898. **24**(4): p. 1-39.
2. Blanchard, G., M. Maunaye, and G. Martin, *Removal of heavy metals from waters by means of natural zeolites*. Water Research, 1984. **18**(12): p. 1501-1507.
3. Roginsky, S. and Y.B. Zeldovich, *The catalytic oxidation of carbon monoxide on manganese dioxide*. Acta Phys. Chem. USSR, 1934. **1**: p. 554.
4. Weber, W.J. and J.C. Morris, *Kinetics of adsorption on carbon from solution*. Journal of the Sanitary Engineering Division, 1963. **89**(2): p. 31-60.
5. Langmuir, *The adsorption of gases on plane surfaces of glass, mica and platinum*. Journal of the American Chemical Society, 1918. **40**(9): p. 1361-1403.
6. Freundlich, H., *Über die adsorption in lösungen*. Zeitschrift für physikalische Chemie, 1907. **57**(1): p. 385-470.
7. Redlich, O. and D.L. Peterson, *A useful adsorption isotherm*. J. Phys. Chem., 1959. **63**: p. 1024.
8. Dubinin, M.M. and L.V. Radushkevich, *Equation of the characteristic curve of activated charcoal*. Chem. Zentr., 1947. **1**: p. 875.
9. Zhou, Q., et al., *Comments on the method of using maximum absorption wavelength to calculate Congo Red solution concentration published in J. Hazard. Mater.* Journal of Hazardous Materials, 2011. **198**: p. 381-382.
10. Lachheb, H., et al., *Photocatalytic degradation of various types of dyes (Alizarin S, Crocein Orange G, Methyl Red, Congo Red, Methylene Blue) in water by UV-irradiated titania*. Applied Catalysis B: Environmental, 2002. **39**(1): p. 75-90.
11. Wahi, R.K., et al., *Photodegradation of Congo Red catalyzed by nanosized TiO<sub>2</sub>*. Journal of Molecular Catalysis A: Chemical, 2005. **242**(1): p. 48-56.
12. Khan, M.I., et al., *Removal of Congo red from aqueous solution by anion exchange membrane (EBTAC): adsorption kinetics and thermodynamics*. Materials, 2015. **8**(7): p. 4147-4161.
13. Machenbach, I., *Membrane technology for dyehouse effluent treatment*. Membrane Technology, 1998. **96**(1998): p. 7-10.
14. Pala, A. and E. Tokat, *Color removal from cotton textile industry wastewater in an activated sludge system with various additives*. Water Research, 2002. **36**(11): p. 2920-2925.
15. Lin, S.H. and M.L. Chen, *Treatment of textile wastewater by chemical methods for reuse*. Water Research, 1997. **31**(4): p. 868-876.
16. Lin, S.H. and C.M. Lin, *Treatment of textile waste effluents by ozonation and chemical coagulation*. Water research, 1993. **27**(12): p. 1743-1748.

17. Beszedits, S., *Ozonation to decolor textile effluents*. American Dyestuff Reporter, 1980. **69**(8): p. 37-&.
18. Gähr, F., F. Hermanutz, and W. Oppermann, *OZONATION – AN IMPORTANT TECHNIQUE TO COMPLY WITH NEW GERMAN LAWS FOR TEXTILE WASTEWATER TREATMENT*. Water Science and Technology, 1994. **30**(3): p. 255-263.
19. Gaehr, F., F. Hermanutz, and W. Oppermann, *Ozonation—an important technique to comply with new German laws for textile wastewater treatment*. Water Science and Technology, 1994. **30**(3): p. 255-263.
20. Kapdan, I.K. and F. Kargi, *Simultaneous biodegradation and adsorption of textile dyestuff in an activated sludge unit*. Process Biochemistry, 2002. **37**(9): p. 973-981.
21. Raval, N.P., P.U. Shah, and N.K. Shah, *Adsorptive amputation of hazardous azo dye Congo red from wastewater: a critical review*. Environmental Science and Pollution Research, 2016. **23**(15): p. 14810-14853.
22. Tran, H.N., S.-J. You, and H.-P. Chao, *Fast and efficient adsorption of methylene green 5 on activated carbon prepared from new chemical activation method*. Journal of Environmental Management 2017. **188**: p. 322-336.
23. Tran, H.N., et al., *Insights into the mechanism of cationic dye adsorption on activated charcoal: the importance of  $\pi$ - $\pi$  interactions*. Process Safety and Environmental Protection, 2017. **107**: p. 168–180.
24. Ledakowicz, S., M. Solecka, and R. Zylla, *Biodegradation, decolourisation and detoxification of textile wastewater enhanced by advanced oxidation processes*. Journal of Biotechnology, 2001. **89**(2): p. 175-184.
25. Galindo, C., P. Jacques, and A. Kalt, *Photodegradation of the aminoazobenzene acid orange 52 by three advanced oxidation processes: UV/H<sub>2</sub>O<sub>2</sub>, UV/TiO<sub>2</sub> and VIS/TiO<sub>2</sub>*. Journal of Photochemistry and Photobiology A: Chemistry, 2000. **130**(1): p. 35-47.
26. Lin, S.H. and C.F. Peng, *Treatment of textile wastewater by electrochemical method*. Water research, 1994. **28**(2): p. 277-282.
27. Laszlo, J.A., *Preparing an ion exchange resin from sugarcane bagasse to remove reactive dye from wastewater*. Textile Chemist & Colorist, 1996. **28**(5).
28. Oladoja, N.A. and A.K. Akinlabi, *Congo Red Biosorption on Palm Kernel Seed Coat*. Industrial & Engineering Chemistry Research, 2009. **48**(13): p. 6188-6196.
29. Bhattacharyya, K.G. and A. Sharma, *Azadirachta indica leaf powder as an effective biosorbent for dyes: a case study with aqueous Congo Red solutions*. Journal of Environmental Management, 2004. **71**(3): p. 217-229.
30. Panda, G.C., S.K. Das, and A.K. Guha, *Jute stick powder as a potential biomass for the removal of congo red and rhodamine B from their aqueous solution*. Journal of Hazardous Materials, 2009. **164**(1): p. 374-379.

31. Wang, X.S. and J.P. Chen, *Biosorption of Congo Red from Aqueous Solution using Wheat Bran and Rice Bran: Batch Studies*. Separation Science and Technology, 2009. **44**(6): p. 1452-1466.
32. Namasivayam, C., et al., *Removal of dyes from aqueous solutions by cellulosic waste orange peel*. Bioresource Technology, 1996. **57**(1): p. 37-43.
33. Annadurai, G., R.-S. Juang, and D.-J. Lee, *Use of cellulose-based wastes for adsorption of dyes from aqueous solutions*. Journal of Hazardous Materials, 2002. **92**(3): p. 263-274.
34. Sewu, D.D., P. Boakye, and S.H. Woo, *Highly efficient adsorption of cationic dye by biochar produced with Korean cabbage waste*. Bioresource Technology, 2017. **224**: p. 206-213.
35. Li, Y., et al., *Production and optimization of bamboo hydrochars for adsorption of Congo red and 2-naphthol*. Bioresource Technology, 2016. **207**: p. 379-386.
36. Nautiyal, P., K.A. Subramanian, and M.G. Dastidar, *Adsorptive removal of dye using biochar derived from residual algae after in-situ transesterification: Alternate use of waste of biodiesel industry*. Journal of Environmental Management, 2016. **182**: p. 187-197.
37. Yang, G., et al., *Removal of Congo Red and Methylene Blue from Aqueous Solutions by Vermicompost-Derived Biochars*. PloS one, 2016. **11**(5): p. e0154562.
38. Dong, Y., et al., *Synthesis of mesoporous carbon fibers with a high adsorption capacity for bulky dye molecules*. Journal of Materials Chemistry A, 2013. **1**(25): p. 7391-7398.
39. Li, J., et al., *Preparation and characterization of high-surface-area activated carbon fibers from silkworm cocoon waste for congo red adsorption*. Biomass and Bioenergy, 2015. **75**: p. 189-200.
40. Kannan, N. and M. Meenakshisundaram, *Adsorption of Congo Red on Various Activated Carbons. A Comparative Study*. Water, Air, and Soil Pollution, 2002. **138**(1): p. 289-305.
41. Purkait, M.K., et al., *Removal of congo red using activated carbon and its regeneration*. Journal of Hazardous Materials, 2007. **145**(1): p. 287-295.
42. Ahmad, R. and R. Kumar, *Adsorptive removal of congo red dye from aqueous solution using bael shell carbon*. Applied Surface Science, 2010. **257**(5): p. 1628-1633.
43. Lei, C., et al., *Superb adsorption capacity of hierarchical calcined Ni/Mg/Al layered double hydroxides for Congo red and Cr(VI) ions*. Journal of Hazardous Materials, 2017. **321**: p. 801-811.
44. Huang, W., X. Yu, and D. Li, *Adsorption removal of Congo red over flower-like porous microspheres derived from Ni/Al layered double hydroxide*. RSC Advances, 2015. **5**(103): p. 84937-84946.

45. Li, J., et al., *Magnetic polydopamine decorated with Mg-Al LDH nanoflakes as a novel bio-based adsorbent for simultaneous removal of potentially toxic metals and anionic dyes*. Journal of Materials Chemistry A, 2016. **4**(5): p. 1737-1746.
46. Ahmed, I.M. and M.S. Gasser, *Adsorption study of anionic reactive dye from aqueous solution to Mg-Fe-CO<sub>3</sub> layered double hydroxide (LDH)*. Applied Surface Science, 2012. **259**: p. 650-656.
47. Shan, R.-r., et al., *Highly efficient removal of three red dyes by adsorption onto Mg-Al-layered double hydroxide*. Journal of Industrial and Engineering Chemistry, 2015. **21**: p. 561-568.
48. Vimonses, V., et al., *Enhancing removal efficiency of anionic dye by combination and calcination of clay materials and calcium hydroxide*. Journal of Hazardous Materials, 2009. **171**(1): p. 941-947.
49. Bulut, E., M. Özacar, and İ.A. Şengil, *Equilibrium and kinetic data and process design for adsorption of Congo Red onto bentonite*. Journal of Hazardous Materials, 2008. **154**(1): p. 613-622.
50. Vimonses, V., et al., *Kinetic study and equilibrium isotherm analysis of Congo Red adsorption by clay materials*. Chemical Engineering Journal, 2009. **148**(2): p. 354-364.
51. Wang, L. and A. Wang, *Adsorption characteristics of Congo Red onto the chitosan/montmorillonite nanocomposite*. Journal of Hazardous Materials, 2007. **147**(3): p. 979-985.
52. Vimonses, V., et al., *Adsorption of congo red by three Australian kaolins*. Applied Clay Science, 2009. **43**(3): p. 465-472.
53. Yang, S., et al., *Enhanced adsorption of Congo red dye by functionalized carbon nanotube/mixed metal oxides nanocomposites derived from layered double hydroxide precursor*. Chemical Engineering Journal, 2015. **275**: p. 315-321.
54. Zhao, J., et al., *Fabrication and Characterization of Highly Porous Fe(OH)<sub>3</sub>@Cellulose Hybrid Fibers for Effective Removal of Congo Red from Contaminated Water*. ACS Sustainable Chemistry & Engineering, 2017.
55. Chatterjee, S., M.W. Lee, and S.H. Woo, *Adsorption of congo red by chitosan hydrogel beads impregnated with carbon nanotubes*. Bioresource Technology, 2010. **101**(6): p. 1800-1806.
56. Wu, Y., H. Luo, and H. Wang, *Efficient Removal of Congo Red from Aqueous Solutions by Surfactant-Modified Hydroxo Aluminum/Graphene Composites*. Separation Science and Technology, 2014. **49**(17): p. 2700-2710.
57. Chatterjee, S., et al., *Enhanced adsorption of congo red from aqueous solutions by chitosan hydrogel beads impregnated with cetyl trimethyl ammonium bromide*. Bioresource Technology, 2009. **100**(11): p. 2803-2809.

58. Wang, L. and A. Wang, *Adsorption properties of congo red from aqueous solution onto N,O-carboxymethyl-chitosan*. Bioresource Technology, 2008. **99**(5): p. 1403-1408.
59. Dhal, J.P., B.G. Mishra, and G. Hota, *Ferrous oxalate, maghemite and hematite nanorods as efficient adsorbents for decontamination of Congo red dye from aqueous system*. International Journal of Environmental Science and Technology, 2015. **12**(6): p. 1845-1856.
60. Pal, S., et al., *Efficient and rapid adsorption characteristics of templating modified guar gum and silica nanocomposite toward removal of toxic reactive blue and Congo red dyes*. Bioresource Technology, 2015. **191**: p. 291-299.
61. Chatterjee, S., T. Chatterjee, and S.H. Woo, *Adsorption of Congo Red from Aqueous Solutions Using Chitosan Hydrogel Beads Formed by Various Anionic Surfactants*. Separation Science and Technology, 2011. **46**(6): p. 986-996.
62. Lei, C., et al., *Hierarchical NiO–SiO<sub>2</sub> composite hollow microspheres with enhanced adsorption affinity towards Congo red in water*. Journal of Colloid and Interface Science, 2016. **466**: p. 238-246.
63. Wang, L. and A. Wang, *Adsorption behaviors of Congo red on the N,O-carboxymethyl-chitosan/montmorillonite nanocomposite*. Chemical Engineering Journal, 2008. **143**(1): p. 43-50.
64. Ansari, M.O., et al., *Anion selective pTSA doped polyaniline@graphene oxide-multiwalled carbon nanotube composite for Cr(VI) and Congo red adsorption*. Journal of Colloid and Interface Science, 2017. **496**: p. 407-415.
65. Zhu, H.Y., et al., *Adsorption removal of congo red onto magnetic cellulose/Fe<sub>3</sub>O<sub>4</sub>/activated carbon composite: Equilibrium, kinetic and thermodynamic studies*. Chemical Engineering Journal, 2011. **173**(2): p. 494-502.
66. Wang, C., Y. Le, and B. Cheng, *Fabrication of porous ZrO<sub>2</sub> hollow sphere and its adsorption performance to Congo red in water*. Ceramics International, 2014. **40**(7): p. 10847-10856.
67. Zhao, X., et al., *Synthesis and characterization of gadolinium doped cobalt ferrite nanoparticles with enhanced adsorption capability for Congo Red*. Chemical Engineering Journal, 2014. **250**: p. 164-174.
68. Shu, J., et al., *Adsorption removal of Congo red from aqueous solution by polyhedral Cu<sub>2</sub>O nanoparticles: Kinetics, isotherms, thermodynamics and mechanism analysis*. Journal of Alloys and Compounds, 2015. **633**: p. 338-346.